

# Elliptic Equations with High-Contrast Coefficients and an Application to Multi-Scale Finite Element Methods

Leonardo A. Poveda<sup>a,\*</sup>, Sebastian Huepo<sup>a</sup>, Victor M. Calo<sup>b</sup>, Juan Galvis<sup>a</sup>

<sup>a</sup>*Departamento de Matemáticas, Universidad Nacional de Colombia, Bogotá D.C., Colombia*

<sup>b</sup>*Applied Mathematics & Computational Science and Earth Sciences & Engineering, King Abdullah University of Science and Technology Thuwal 23955-6900 Kingdom of Saudi Arabia*

---

## Abstract

In this paper we design a multiscale finite element method using asymptotic expansions for elliptic equations with high-contrast coefficients applying recent results on the approximation of solutions of such equations. In particular, we use an asymptotic expansion of the solution for the case multiple high-conductivity inclusions. An important contribution is that we use a modification of the expansion that uses only local solutions to construct basis functions. In this case, we approximate the limit of the asymptotic expansion with a similar expansion constructed with localized harmonic characteristic functions. We present some representative numerical examples that confirm the theory.

*Keywords:* Elliptic equation, asymptotic expansions, high-contrast coefficients, multiscale method, harmonic characteristic function.

---

\*Corresponding author at: Departamento de Matemáticas, Universidad Nacional de Colombia, Bogotá, D.C.

*Email addresses:* leapovedacu@unal.edu.co (Leonardo A. Poveda), shuepobe@unal.edu.co (Sebastian Huepo), victor.calo@kaust.edu.sa (Victor M. Calo), jcgaltisa@unal.edu.co (Juan Galvis)

---

## 1. Introduction

Many problems come from various physical and engineering applications which naturally have multiscale solutions. For instance, problems related to composite materials and porous media flows. The mathematical and numerical analysis for these problems are very challenging since they are governed by elliptic equations with high-contrast coefficients Hou and Wu (1997); Chen and Hou (2003); Galvis and Efendiev (2010). For example, in many applications related to fluid flows in porous media, the coefficient in the equation models the permeability (which represents how easy the porous media let the fluid flow). The values of the permeability usual and specially for complicated porous media, vary in several orders of magnitude. We refer to this case as the high-contrast case and we say that the corresponding elliptic equation that models (e.g., the pressure) has high-contrast coefficients; see for instance Galvis and Ki Kang (2014); Efendiev et al. (2013); Efendiev and Galvis (2012).

A fundamental aim is to understand the effects on the solution related to the variations of high-contrast in the properties of the porous media. In terms of the model, these variations appear in the coefficients of the differential equations. We consider a previous work by Calo et al. (2014), where authors report some results on the asymptotic expansion for the solution. The asymptotic expansion is obtained in terms of the high-contrast in the coefficient.

Our goal is to further analyze the expansion introduced in Calo et al. (2014) and use it to design numerical strategies to approximate solutions. In

particular, we consider the derivation for multiple high-conductivity inclusions only for the first term of the expansion (others terms of the expansion are computed similarly). We modify the computation so that instead of using the harmonic characteristic function in whole domain (the background and inclusions) we use the harmonic characteristic function in a local domain. This fact is very important in computational terms considering that the computation of the harmonic characteristic function is computationally expensive at the time of showing numerical solutions.

We mention that the asymptotic expansion helps to design numerical strategies and also has other applications. In order to devise efficient numerical strategies, we use the expansion to better understand the behavior of solutions when restricted to local domains. In addition, the nature of the asymptotic expansion will reveal properties of the solution. For instance, we can compute functionals of solutions and single out their behavior with respect to the contrast or other important parameters.

The rest of the paper is organized as follows. In Section 2 we introduce the problem setting. In Section 3 we recall the derivation of the expansion for multiple high-conductivity inclusions. We also introduce the definition of harmonic characteristic functions, which help us to determinate the function leading term of the expansion and its behavior in the background and inclusions. Section 4 is dedicated to the application to Multiscale Finite Elements, in particular we consider the approximation of leading term of the expansion with localized harmonic characteristic function. This approximation is considered for the case of many (highly dense) high-contrast inclusions. In Section 5 we present some numerical experiments of the resulting methods.

Finally, in Section 6 we state some conclusions and final comments.

## 2. Problem Setting

In this section, we use the notation introduced in Calo et al. (2014). We take the derivation of asymptotic expansions for high-contrast elliptic problems of the form,

$$-\operatorname{div}(\kappa \operatorname{grad} u) = f, \quad \text{in } D, \quad (1)$$

with Dirichlet data defined by  $u = g$  on  $\partial D$ . We assume that  $D$  is the disjoint union of a background domain and inclusions, i.e.,  $D = D_0 \cup (\bigcup_{m=1}^M \overline{D}_m)$ . We assume that  $D_0, D_1, \dots, D_M$  are polygonal domains (or domains with smooth boundaries). We also assume that each  $D_m$  is a connected domain,  $m = 0, 1, \dots, M$ . Additionally, we consider that  $D_m$  is compactly included in the open set  $D \setminus \bigcup_{\ell=1, \ell \neq m}^M \overline{D}_\ell$ , i.e.,  $\overline{D}_m \subset D \setminus \bigcup_{\ell=1, \ell \neq m}^M \overline{D}_\ell$ , and we define  $D_0 := D \setminus \bigcup_{m=1}^M \overline{D}_m$ . Let  $D_0$  represent the background domain and the subdomains  $\{D_m\}_{m=1}^M$  represent inclusions. For simplicity of the presentation we consider only interior inclusions. Other cases can be studied similarly.

We consider a coefficient with multiple high-conductivity inclusions. Let  $\kappa$  be defined by

$$\kappa(x) = \begin{cases} \eta, & x \in D_m, \quad m = 1, \dots, M, \\ 1, & x \in D_0 = D \setminus \bigcup_{m=1}^M \overline{D}_m. \end{cases} \quad (2)$$

We seek to determine  $\{u_j\}_{j=0}^\infty \subset H^1(D)$  such that

$$u_\eta = u_0 + \frac{1}{\eta} u_1 + \frac{1}{\eta^2} u_2 + \dots = \sum_{j=0}^{\infty} \eta^{-j} u_j, \quad (3)$$

and such that they satisfy the following Dirichlet boundary conditions,

$$u_0 = g \text{ on } \partial D \quad \text{and} \quad u_j = 0 \text{ on } \partial D \text{ for } j \geq 1. \quad (4)$$

We have the following weak formulation of problem (1): find  $u \in H^1(D)$  such that

$$\begin{cases} \mathcal{A}(u, v) = \mathcal{F}(v), & \text{for all } v \in H_0^1(D), \\ u = g, & \text{on } \partial D. \end{cases} \quad (5)$$

The bilinear form  $\mathcal{A}$  and the linear functional  $\mathcal{F}$  are defined by

$$\begin{aligned} \mathcal{A}(u, v) &= \int_D \kappa(x) \nabla u(x) \cdot \nabla v(x) dx, \text{ for all } u, v \in H_0^1(D) \\ \mathcal{F}(v) &= \int_D f(x) v(x) dx, \text{ for all } v \in H_0^1(D). \end{aligned} \quad (6)$$

We denote by  $u_\eta$  the solution of problem (5) with Dirichlet boundary condition (4). From now on, we use the notation  $w^{(m)}$ , which means that the function  $w$  is restricted on domain  $D_m$ , that is  $w^{(m)} = w|_{D_m}$ ,  $m = 0, 1, \dots, M$ .

### 3. Derivation for Multiple High-Conductivity Inclusions

In this section we take results of the asymptotic problems from Calo et al. (2014). We consider the case of multiply high-conductivity inclusions. Define the space of constant functions inside the inclusions

$$V_{const} = \{v \in H_0^1(D), \text{ such that } v|_{D_m} \text{ is a constant for all } m = 1, \dots, M\}.$$

It is easy to see that  $u_0$  (the asymptotic limit of the solution when  $\eta \rightarrow \infty$ ) is constant inside the inclusions. If we choose the test function  $z \in V_{const}$  in (5) we see that  $u_0$  satisfies the problem

$$\begin{aligned} \int_{D_0} \nabla u_0 \cdot \nabla z &= \int_D f z, \quad \text{for all } z \in V_{const} \\ u_0 &= g, \quad \text{on } \partial D. \end{aligned} \quad (7)$$

The problem (7) is elliptic and it has a unique solution, see Calo et al. (2014). For each  $m = 1, \dots, M$  we introduce the *harmonic characteristic function*  $\chi_{D_m} \in H_0^1(D)$  with the condition

$$\chi_{D_m}^{(1)} \equiv \delta_{m\ell} \text{ in } D_\ell, \text{ for } \ell = 1, \dots, M, \quad (8)$$

and which is equal to the harmonic extension of its boundary data in  $D_0$ ,  $\chi_{D_m}$  (see Calo et al. (2014)). We then have,

$$\begin{cases} \int_{D_0} \nabla \chi_m \cdot \nabla v = 0, & \text{for } v \in H_0^1(D_0) \\ \chi_m = 0, & \text{on } \partial D \text{ and } \partial D_\ell, m \neq \ell, \ell = 1, 2, \dots, M \\ \chi_m = 1, & \text{on } \partial D_m, \end{cases} \quad (9)$$

Where  $\delta_{m\ell}$  represent the Kronecker delta, which is equal to 1 when  $m = \ell$  and 0 otherwise. To obtain an explicit formula for  $u_0$  we use the facts that the problem (9), which is elliptic and has unique solution (and some property of the harmonic characteristic functions described in Calo et al. (2014)).

We decompose  $u_0$  into the harmonic extension to  $D_0$  of a function in  $V_{const}$  plus a function  $u_{0,0}$  with value  $g$  on  $\partial D$  and zero on  $\partial D_m$ ,  $m = 1, \dots, M$ . We write

$$u_0 = u_{0,0} + \sum_{m=1}^M c_m(u_0) \chi_{D_m},$$

where  $u_{0,0} \in H^1(D)$  with  $u_{0,0} = 0$  in  $D_m$  for  $m = 1, \dots, M$ , and  $u_{0,0}$  solves the problem in  $D_0$

$$\int_{D_0} \nabla u_{0,0} \cdot \nabla z = \int_{D_0} f z, \quad \text{for all } z \in H_0^1(D_0), \quad (10)$$

with  $u_{0,0} = 0$  on  $\partial D_m$ ,  $m = 1, \dots, M$  and  $u_{0,0} = g$  on  $\partial D$ . We have

$$\int_{D_0} \nabla \left( u_{0,0} + \sum_{m=1}^M c_m(u_0) \chi_{D_m} \right) \cdot \nabla \chi_{D_\ell} = \int_D f \chi_{D_\ell}, \quad \text{for } \ell = 1, \dots, M,$$

or

$$\sum_{m=1}^M c_m(u_0) \int_{D_0} \nabla \chi_{D_m} \cdot \nabla \chi_{D_\ell} = \int_D f \chi_{D_\ell} - \int_{D_0} \nabla u_{0,0} \cdot \nabla \chi_{D_\ell},$$

and the problem above is equivalent to the linear system,

$$\mathbf{A}_{geom} \mathbf{X} = \mathbf{b},$$

where  $\mathbf{A}_{geom} = [a_{m\ell}]$  and  $\mathbf{b} = (b_1, \dots, b_M) \in \mathbb{R}^M$  are defined by

$$a_{m\ell} = \int_D \nabla \chi_{D_m} \cdot \nabla \chi_{D_\ell} = \int_{D_0} \nabla \chi_{D_m} \cdot \nabla \chi_{D_\ell}, \quad (11)$$

$$b_\ell = \int_D f \chi_{D_\ell} - \int_{D_0} \nabla u_{0,0} \cdot \nabla \chi_{D_\ell}, \quad (12)$$

and  $\mathbf{X} = (c_1(u_0), \dots, c_M(u_0)) \in \mathbb{R}^M$ . Then we have

$$\mathbf{X} = \mathbf{A}_{geom}^{-1} \mathbf{b}. \quad (13)$$

Now using the definition given for  $\chi_{D_m}$  we have

$$a_{m\ell} = \int_D \nabla \chi_{D_m} \cdot \nabla \chi_{D_\ell} = \int_{\partial D_m} \chi_{D_\ell} \cdot n_m = \int_{\partial D_\ell} \nabla \chi_{D_\ell} \cdot n_\ell. \quad (14)$$

Note that  $\sum_{m=1}^M c_m(u_0) \chi_{D_m}$  is a Galerkin projection in the space  $\text{Span} \{\chi_{D_m}\}_{m=1}^M$ .

For more details see Calo et al. (2014).

Now for the sake of completeness, we describe the next individual terms of the asymptotic expansion. We have the restriction of  $u_1$  to the sub-domain  $D_m$ , that is

$$u_1^{(m)} = \tilde{u}_1^{(m)} + c_{1,m}, \quad \text{with} \quad \int_{D_m} \tilde{u}_1^{(m)} = 0,$$

and  $\tilde{u}_1^{(m)}$  satisfies the Neumann problem

$$\int_{D_m} \nabla \tilde{u}_1^{(m)} \cdot \nabla z = \int_{D_m} f z - \int_{\partial D_m} \nabla u_0^{(0)} \cdot n_m z, \quad \text{for all } z \in H^1(D_m),$$

for  $m = 1, \dots, M$ . To obtain in detail the constants  $c_{1,m}$ ; see Calo et al. (2014).

Now, for  $j = 1, 2, \dots$  we have that  $u_j^{(m)}$  in  $D_m$ ,  $m = 1, \dots, M$ , then we find  $u_j^{(0)}$  in  $D_0$  by solving the Dirichlet problem

$$\begin{aligned} \int_{D_0} \nabla u_j^{(0)} \cdot \nabla z &= 0, \text{ for all } z \in H_0^1(D_0) \\ u_j^{(0)} &= u_j^{(m)} \left( = \tilde{u}_j^{(m)} + c_{j,m} \right), \text{ on } \partial D_m, m = 1, \dots, M, \\ u_j^{(0)} &= 0, \text{ on } \partial D. \end{aligned} \tag{15}$$

Since  $c_{j,m}$  are constants, we define their corresponding harmonic extension by  $\sum_{m=1}^M c_{j,m} \chi_{D_m}$ . So we rewrite

$$u_j = \tilde{u}_j + \sum_{m=1}^M c_{j,m} \chi_{D_m}. \tag{16}$$

The  $u_{j+1}^{(m)}$  in  $D_m$  satisfy the following Neumann problem

$$\int_{D_m} \nabla u_{j+1}^{(m)} \cdot \nabla z = - \int_{\partial D_m} \nabla u_j^{(0)} \cdot n_0 z, \quad \text{for all } z \in H^1(D).$$

The compatibility condition is satisfied; see Calo et al. (2014), then we have that

$$\begin{aligned} 0 = \int_{\partial D_\ell} \nabla u_{j+1}^{(\ell)} \cdot n_\ell &= - \int_{\partial D_\ell} \nabla u_j^{(0)} \cdot n_0 \\ &= - \int_{\partial D_\ell} \nabla \left( \tilde{u}_j^{(0)} + \sum_{m=1}^M c_{j,m} \chi_{D_m}^{(0)} \right) \cdot n_0 \\ &= - \int_{\partial D_\ell} \nabla \tilde{u}_j^{(0)} \cdot n_0 - \sum_{m=1}^M c_{j,m} \int_{\partial D_m} \nabla \chi_{D_m}^{(0)} \cdot n_0. \end{aligned}$$

From (11) and (14) we have that  $\mathbf{X}_j = (c_{j,1}, \dots, c_{j,M})$  is the solution of the system

$$\mathbf{A}_{geom} \mathbf{X}_j = \mathbf{Y}_j,$$



where

$$\mathbf{Y}_j = \left( - \int_{\partial D_1} \nabla \tilde{u}_j^{(0)} \cdot n_0, \dots, - \int_{\partial D_m} \nabla \tilde{u}_j^{(0)} \cdot n_0 \right),$$

or

$$\mathbf{Y}_j = \left( - \int_{D_0} \nabla \tilde{u}_j^{(0)} \cdot \nabla \chi_{D_1}, \dots, - \int_{D_0} \nabla \tilde{u}_j^{(0)} \cdot \nabla \chi_{D_M} \right).$$

For the convergence we have the result obtained in Calo et al. (2014). It is shown if there are constants  $C, C_1 > 0$  such that  $\eta > C$ , the expansion (3) converges absolutely in  $H^1(D)$  for  $\eta$  sufficiently large. We recall the following result.

**Theorem 1.** *Consider the problem (5) with coefficient (2). The corresponding expansion (3) with boundary condition (4) converges absolutely in  $H^1(D)$  for  $\eta$  sufficiently large. Moreover, there exist positive constants  $C$  and  $C_1$  such that for every  $\eta > C$ , we have*

$$\left\| u - \sum_{j=0}^J \eta^{-j} u_j \right\|_{H^1(D)} \leq C_1 (\|f\|_{H^{-1}(D)} + \|g\|_{H^{1/2}(\partial D)}) \sum_{j=J+1}^{\infty} \left( \frac{C}{\eta} \right)^j,$$

for  $J \geq 0$ .

For a proof we refer to Calo et al. (2014).

#### 4. Applications to Multiscale Finite Elements: Approximation of $u_0$ with Localized Harmonic Characteristic

In this section we present some numerical studies. We assume that  $D$  is the union of a background and multiple inclusions homogeneously distributed. Other more general cases can also be considered. In particular, we consider one approximation of the leading term  $u_0$  with localized harmonic

characteristics. This is motivated due to the fact that, the computation of the harmonic characteristic functions is computationally expensive. One option is to approximate harmonic characteristics functions by solving a local problem (instead of a whole background problem). For instance, the domain where a harmonic characteristic functions can computed. This is illustrated in Figure 1, where the approximated harmonic characteristic function will be zero on the boundary of the neighborhood of the selected inclusion (green color).

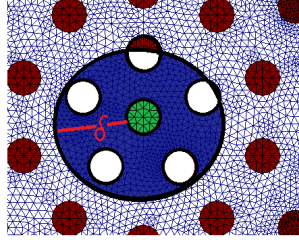


Figure 1: Illustration of  $\delta$ - neighborhood of an inclusion. The selected inclusion is marked with green color. We show in blue color the  $\delta$ -neighborhood of this inclusion. We highlighted with white color the other inclusions that are within the  $\delta$ -neighborhood of the selected inclusion.

We know that the harmonic characteristic function are defined by solving a problem in the background, which is a global problem. The idea is then to solve a similar problem only a neighborhood of each inclusion. The exact characteristic functions are defined by (9). We define the neighborhood of the inclusion  $D_m$ , by

$$D_{m,\delta} = \overline{D}_m \cup \{x \in D_0 : d(x, D_m) < \delta\}, \quad (\text{see Figure 1}),$$

and we define the characteristic function for the  $\delta$ -neighborhood by

$$\begin{cases} \int_D \nabla \chi_m^\delta \cdot \nabla v = 0, & \text{for } v \in H_0^1(D_{m,\delta}) \\ \chi_m^\delta = 0, & \text{on } \partial D_{m,\delta} \text{ and } \partial D_\ell \cap D_{m,\delta} \text{ for } \ell \neq m, \\ \chi_m^\delta = 1, & \text{on } \partial D_m. \end{cases} \quad (17)$$

We remind that the exact expression for  $u_0$  is given by

$$u_0 = u_{0,0} + \sum_{m=1}^M c_m \chi_{D_m} = u_{0,0} + u_c, \quad (18)$$

where we have introduced  $u_c = \sum_{m=1}^M c_m(u_0) \chi_{D_m}$ . The matrix problem for  $u_c$  with globally supported basis is then,

$$\mathbf{A} \mathbf{c} = \mathbf{b},$$

with  $\mathbf{A} = [a_{m\ell}]$ , with  $a_{m\ell} = \int_{D_m} \nabla \chi_m \cdot \nabla \chi_\ell$ ,  $\mathbf{c} = [c_0(u_0), \dots, c_M(u_0)]$  and  $\mathbf{b} = [b_\ell] = \int_D f \chi_{D_\ell}$ . Define  $u_0^\delta$  using similar expression given by

$$u_0^\delta = u_{0,0}^\delta + \sum_{m=1}^M c_m^\delta \chi_{D_m}^\delta = u_{0,0}^\delta + u_c^\delta, \quad (19)$$

where  $c_m^\delta$  is computed similarly to  $c_m$  using an alternative matrix problem with basis  $\chi_{D_m}^\delta$  instead of  $\chi_{D_m}$ . This system is given by

$$\mathbf{A}^\delta \mathbf{c}^\delta = \mathbf{b}^\delta.$$

with  $\mathbf{A}^\delta = [a_{m\ell}^\delta]$ , with  $a_{m\ell}^\delta = \int_{D_m} \nabla \chi_m^\delta \cdot \nabla \chi_\ell^\delta$ ,  $\mathbf{c}^\delta = [c_0^\delta(u_0), \dots, c_M^\delta(u_0)]$  and  $\mathbf{b}^\delta = [b_\ell^\delta] = \int_D f \chi_{D_\ell}^\delta$ .

We also introduced the  $u_{0,0}^\delta$  that is an approximation to  $u_{0,0}$ , that solves the problem

$$\begin{aligned} \int_{D_0^\delta} \nabla u_{0,0}^\delta \cdot \nabla v &= \int_{D_0^\delta} f v, \text{ for all } v \in H_0^1(D_0^\delta) \\ u_{0,0}^\delta &= g, \text{ on } \partial D \\ u_{0,0}^\delta &= 0, \text{ on } \partial D_0^\delta \cap D \text{ and } \partial D_0^\delta \setminus \partial D, \end{aligned}$$

where

$$D_0^\delta = \{x \in D : d(x, \partial D) < \delta\}.$$

We use the numerical implementation for this case and show two numerical examples in the Section below.

## 5. Numerical Experiments

In this section we show some examples of the expansion terms in two dimensions. We use MATLAB for the computations. In particular, few terms are computed numerically using a Finite Elements Method. For details on the Finite Element Methods, see for instance Johnson (2009); Galvis (2009). See also Das et al. (1994) for some other numerical method.

We recall that, our main goal is to devise efficient numerical approximations for  $u_0$  (and then for  $u_\eta$  by using Theorem 1).

### 5.1. Example 1: 36 Inclusions

We consider  $D = B(0, 1)$  the circle with center  $(0, 0)$ , radius 1 and 36 (identical) circular inclusions of radius 0.07, this is illustrated in the Figure 2 (left side). Then we numerically solve the problem

$$\begin{cases} -\operatorname{div}(\kappa(x)\nabla u_\eta(x)) = 1, & \text{in } D \\ u(x) = x_1 + x_2^2, & \text{on } \partial D. \end{cases} \quad (20)$$

We show in Figure 2 an approximation for function  $u_0$  with  $\eta = 6$ . For this case we have the behavior of the term  $u_0$  inside the background. We refer to the term  $u_c$  for the number of inclusions present in the geometry of problem (20).

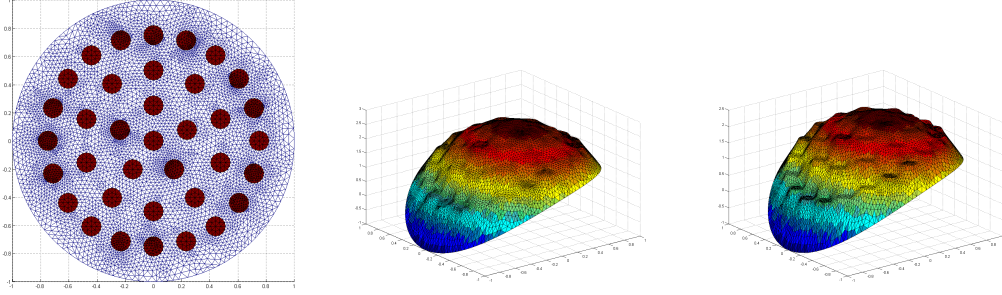


Figure 2: Geometry of the problem (20) with  $\eta = 6$ . Asymptotic solution  $u_0 = u_{00} + u_c$  homogeneously

In Figure 3 we show the behavior of functions  $u_0$  (right side) and  $u_{0,0}$  (left side) in the background with coefficient  $\eta = 10$ , which is defined in (2) for the problem (20).

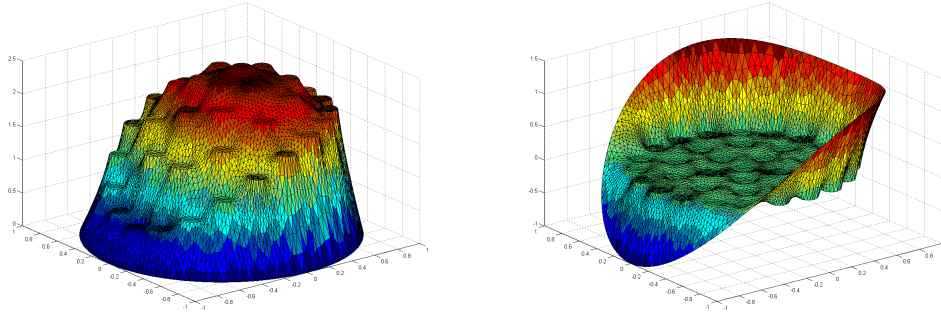


Figure 3: Behavior of individual functions  $u_0$  and  $u_{0,0}$  inside the background for the problem (20) with  $\eta = 10$ .

In Figure 4, we show the computed two terms  $u_1$  and  $u_2$  of the asymptotic expansion. We plot of functions  $u_1$  and  $u_2$  (Top). We also show the same functions only restricted to the inclusions (Bottom).

An interesting case for different values of  $\eta$  and the number of terms

needed to obtain the relative error of the approximation is reported in the Table 1. We observe that for problem (20) it is necessary (for instance with a value of  $\eta = 10^8$ ) to use only one term of the expansion to achieve a relative error of the order of  $10^{-8}$ .

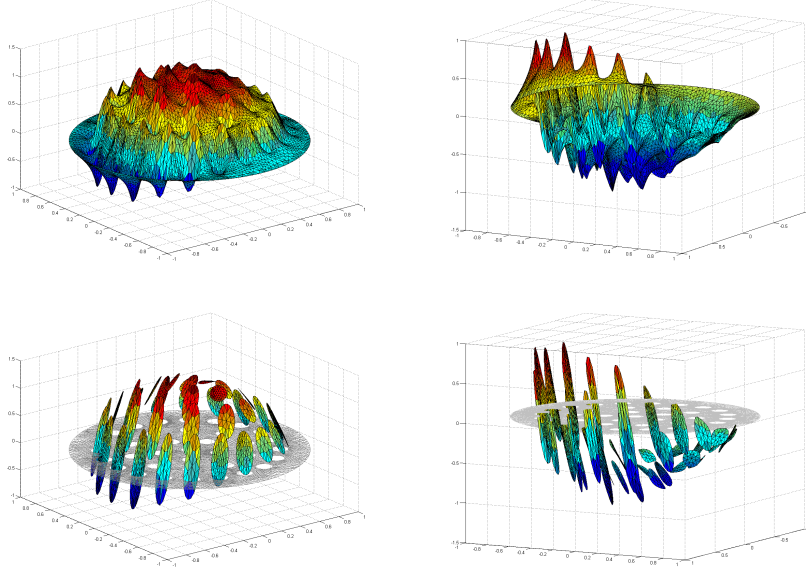


Figure 4: Top: Functions  $u_1$  and  $u_2$ . Bottom: Functions  $u_1$  and  $u_2$  restricted to the inclusions.

$\eta$	3	4	5	6	7	8	9	10	$10^2$	$10^3$	$10^4$	$10^5$	$10^6$	$10^7$	$10^8$
#	25	16	13	11	10	9	8	8	4	3	2	2	2	1	1

Table 1: Number of terms needed to obtain a relative error of  $10^{-8}$  for a given value of  $\eta$ .

### 5.1.1. Approximation of $u_0$ using localized harmonic characteristics

We consider again the geometry of the previous subsection and study the expansion with localized harmonic characteristic functions. In Figure 5 we plot the globally characteristic function (left side) in one inclusion. We observe that the harmonic characteristic function is zero on boundary of all other inclusions. In addition, we also plot the difference between the localized characteristic function in (17) and the characteristic function in (9); see Figure 5, right picture. Here we use  $\delta = 0.3$  and observe that the maximum value of this difference is 0.016.

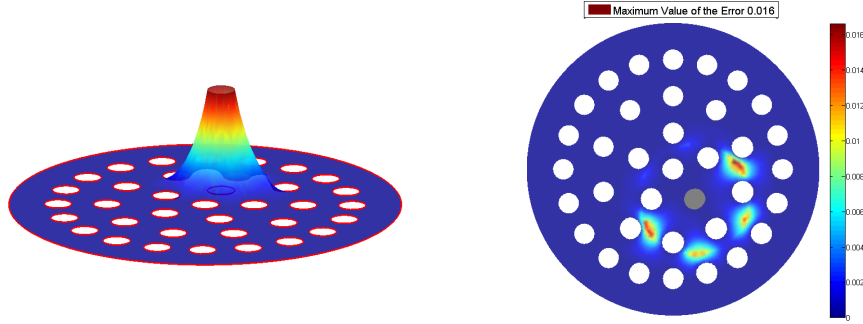


Figure 5: Left picture: Illustration of the Globally characteristic function for the problem (20). Right picture: difference between the globally characteristic function (9) and the Localized characteristic function (17) . Here we use  $\delta = 0.3$  and maximum value of the difference is 0.016.

We have the numerical results for the different values of  $\delta$  in the Table 2. We solve for the harmonic characteristic function with zero Dirichlet boundary condition within a distance  $\delta$  of the boundary of the inclusion.

The relative  $H^1$  error that relates the exact leading term of the asymptotic

$\delta$	$e(u_0 - u_0^\delta)$	$e(u_{0,0} - u_{0,0}^\delta)$	$e(u_c - u_c^\delta)$
0.001000	0.830673	0.999907	0.555113
0.050000	0.530459	0.768135	0.549068
0.100000	0.336229	0.639191	0.512751
0.200000	0.081500	0.261912	0.216649
0.300000	0.044613	0.088706	0.048173
0.400000	0.041061	0.047743	0.007886
0.500000	0.033781	0.034508	0.001225
0.600000	0.029269	0.029362	0.000174
0.700000	0.020881	0.020888	0.000021
0.800000	0.012772	0.012773	0.000003
0.900000	0.006172	0.006172	0.000000

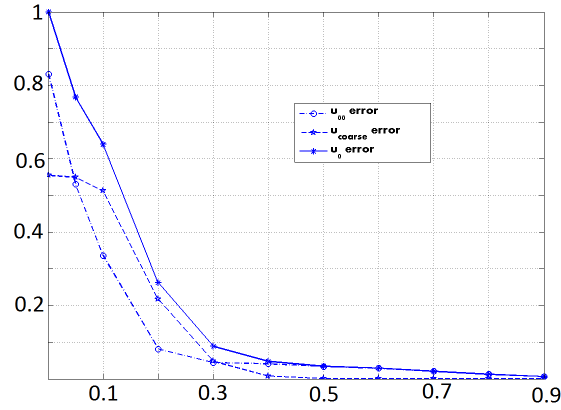


Table 2: Relative error in the approximation of  $u_0$  by using locally computed basis functions and truncated boundary condition effect.  $e(w) = \|w\|_{H^1}/\|u_0\|_{H^1}$ . Here  $u_0 = u_{0,0} + u_c$  where  $u_c$  is combination of harmonic characteristic functions and  $u_0^\delta = u_{0,0}^\delta + u_c^\delta$  is computed by solving  $u_{0,0}^\delta$  on a  $\delta$ -strip of the boundary  $\partial D$  and the basis functions on a  $\delta$ -strip of the boundary of each inclusion.



expansion, that is  $u_0$  in (18), and its approximation  $u_0^\delta$  in (19), is given by

$$e(u_0 - u_0^\delta) = \frac{\|u_0 - u_0^\delta\|_{H^1}}{\|u_0\|_{H^1}}.$$

Analogously, the relative  $H^1$  error of the approximation of  $u_{0,0}$  is given by

$$e(u_{0,0} - u_{0,0}^\delta) = \frac{\|u_{0,0} - u_{0,0}^\delta\|_{H^1}}{\|u_{0,0}\|_{H^1}}.$$

The error  $e(u_c - u_c^\delta)$  is defined in a similar way.

We recall that, according to Theorem 1, the error between the exact solution of problem (5) with coefficient (2) and  $u_0$  in (18) is of order  $\frac{1}{\eta}$  and it is not presented here.

In the Table 2 we observe that as the neighborhood becomes bigger, the error is smaller. For instance, if we have a  $\delta = 0.2$ , the error that relates the exact solution  $u_0$  and the truncated solution  $u_0^\delta$  is around 8%. In analogous way an error presents around 6% between the function  $u_{0,0}$  and  $u_{0,0}^\delta$ .

### 5.2. Example 2: 60 Inclusions

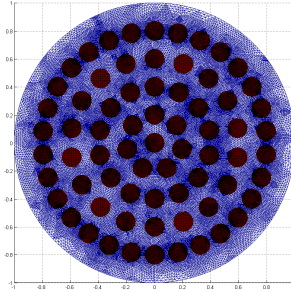


Figure 6: Geometry for the problem (21).

Similarly, we study of the expansion with  $\chi$  in  $D = (0, 1)$  the circle with center  $(0, 0)$ , radius 1 and 60 (identical) circular inclusions of radius 0.07.

We numerically solve the following problem

$$\begin{cases} -\operatorname{div}(\kappa(x)\nabla u_\eta(x)) = 1, & \text{in } D \\ u(x) = x_1 + x_2^2, & \text{on } \partial D, \end{cases} \quad (21)$$

In the Figure 6 we illustrate the geometry for the problem (21). We have the similar numeric results for the different values of  $\delta$  in the Table 3 for the problem (21). We solve for the harmonic characteristic function with zero Dirichlet boundary condition within a distance  $\delta$  of the boundary of the inclusion.

#### 5.2.1. Approximation of $u_0$ using localized harmonic characteristics

For this example we have a difference in the numerically analysis to the problem (20) in the Section 5.1 it is due to numbers inclusions presents in the problem (21). In the Table 3 we observe that as the neighborhood approximates total domain, its error is relatively small. For instance, if we have a  $\delta = 0.20000$ , the error that relates the exact solution  $u_0$  and the truncated solution  $u_0^\delta$  is around 1%. The relative error is 2% between the function  $u_{0,0}$  and  $u_{0,0}^\delta$ .

We state that if there are several high-conductivity inclusions in the geometry, which are closely distributed, the localized harmonic characteristic function decay rapidly to zero for any  $\delta$ -neighborhood.

## 6. Conclusions and Final Comments

We presented and overview of the computation of the asymptotic expansion for high-contrast problems. The asymptotic expansion is written in terms of the contrast  $\eta$ . In particular, using the expansion we design

$\delta$	$e(u_0 - u_0^\delta)$	$e(u_{00} - u_{0,0}^\delta)$	$e(u_c - u_c^\delta)$
0.001000	0.912746	0.999972	0.408063
0.050000	0.369838	0.549332	0.399472
0.100000	0.181871	0.351184	0.258946
0.200000	0.013781	0.020172	0.011061
0.300000	0.013332	0.013433	0.000737
0.400000	0.010394	0.010396	0.000057
0.500000	0.009228	0.009228	0.000004
0.600000	0.006102	0.006102	0.000000
0.700000	0.005561	0.005561	0.000000
0.800000	0.002239	0.002239	0.000000
0.900000	0.001724	0.001724	0.000000

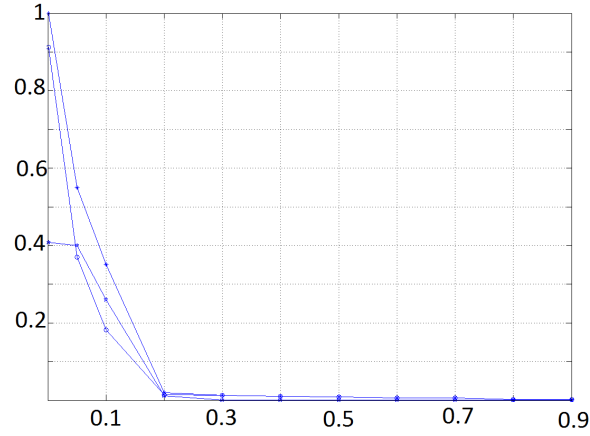


Table 3: Relative error in the approximation of  $u_0$  by using locally computed basis functions and truncated boundary condition effect.  $e(w) = \|w\|_{H^1}/\|u_0\|_{H^1}$ . Here  $u_0 = u_{0,0} + u_c$  where  $u_c$  is combination of harmonic characteristic functions and  $u_0^\delta = u_{0,0}^\delta + u_c^\delta$  is computed by solving  $u_{0,0}^\delta$  on a  $\delta$ -strip of the boundary  $\partial D$  and the basis functions on a  $\delta$ -strip of the boundary of each inclusion.

multiscale method for the approximation of the asymptotic limit. A main application is to find procedures to quickly compute the first few terms in the expansion. In particular, the asymptotic limit, which, as seen in the manuscript, it is an approximation of order  $\eta^{-1}$  to the solution. The main idea of the method is to approximate the harmonic characteristic functions by solving a local problem (instead of a whole background problem). We gave some numerical examples of the computation of the term  $u_0$  with the localized harmonic characteristic function. The analysis of the truncation error depends on decay properties of the harmonic characteristic functions and its under current investigations. This method can be also applied to several interesting models with heterogeneous coefficients and explicit application will also be consider in the future.

## References

- Calo, V. M., Efendiev, Y., Galvis, J., 2014. Asymptotic expansions for high-contrast elliptic equations. *Math. Models Methods Appl. Sci* 24, 465–494.
- Chen, Z., Hou, T., 2003. A mixed multiscale finite element method for elliptic problems with oscillating coefficients. *Mathematics of Computation* 72 (242), 541–576.
- Das, B., Steinberg, S., Weber, S., Schaffer, S., 1994. Finite difference methods for modeling porous media flows. *Transport in Porous Media* 17 (2), 171–200.
- Efendiev, Y., Galvis, J., 2012. Coarse-grid multiscale model reduction tech-

- niques for flows in heterogeneous media and applications. In: Numerical Analysis of Multiscale Problems. Springer, pp. 97–125.
- Efendiev, Y., Galvis, J., Hou, T. Y., 2013. Generalized multiscale finite element methods (gmsfem). *Journal of Computational Physics* 251, 116–135.
- Galvis, J., 2009. Introdução aos métodos de decomposição de domínio. Lecture notes for a minicourse in the 27 Colóquio Brasileiro de Matemática IMPA.
- Galvis, J., Efendiev, Y., 2010. Domain decomposition preconditioners for multiscale flows in high-contrast media. *Multiscale Modeling & Simulation* 8 (4), 1461–1483.
- Galvis, J., Ki Kang, S., 2014. Spectral multiscale finite element for nonlinear flows in highly heterogeneous media: A reduced basis approach. *Journal of Computational and Applied Mathematics* 260, 494–508.
- Hou, T. Y., Wu, X.-H., 1997. A multiscale finite element method for elliptic problems in composite materials and porous media. *Journal of computational physics* 134 (1), 169–189.
- Johnson, C., 2009. Numerical solution of partial differential equations by the finite element method. Dover Publications, Inc., Mineola, NY, reprint of the 1987 edition.